Transfer and compound-nucleus reactions that lead to the nuclei ^{245}Cf and ^{244}Cf: Interactions of ^{12}C with ^{239}Pu and ^{238}U

R. L. Hahn,* P. F. Dittner, K. S. Toth, and O. L. Keller
Oak Ridge National Laboratory,† Oak Ridge, Tennessee 37830
(Received 28 May 1974)

The nuclear reactions ^{239}Pu(^{12}C, $\alpha 2n$-$\alpha 3n$) and ^{238}U(^{12}C, $5n$-$6n$) leading to the same radioactive products ^{245}Cf and ^{244}Cf have been studied by measuring excitation functions and recoil range and angular distributions. As expected, the U + C data are consistent with predictions for complete-fusion (CF) reactions; for example, the range distributions are Gaussian with mean values that increase with increasing bombarding energy, and the angular distributions are forward peaked in the laboratory system. The results for the Pu + C reactions differ markedly from those for U + C. The range distributions are asymmetric, with high energy tails, and have centroids that decrease monotonically with increasing ^{12}C energy, from 1.6 times the expected CF value at 67 MeV to 0.6 of the CF value at 97 MeV; the angular distributions are characterized by a maximum at $\sim 17°$ (lab) at energies well above the Coulomb barrier. The cross sections for the Pu(C, $\alpha 2n$ and $\alpha 3n$) reactions are much larger than those of the Pu(C, $2n$ to $4n$) reactions, also indicating that noncompound processes are involved in the production of the Cf nuclides, since evaporation of charged particles is expected to be negligible in such heavy nuclei. All of these results for the (C, αxn) reactions are consistent with models of transfer reactions in which an aggregate is transferred from the projectile to the target nucleus, followed by evaporation of neutrons from the resulting heavy nucleus. In particular, the average recoil energies and angles are reproduced reasonably well by models that consider the kinematics of the transfer process.

[NUCLEAR REACTIONS ^{239}Pu(^{12}C, $\alpha 2n$ and $\alpha 3n$) and ^{238}U(^{12}C, $5n$ and $6n$). E = 63–97 MeV; measured $\sigma(E)$, recoil range and angular distributions for ^{245}Cf and ^{244}Cf; deduced average values of ranges, recoil energies E_R and angles of emission θ_R; calculated E_R and θ_R with models of transfer reactions.]

I. INTRODUCTION

The possibility of the transfer of many nucleons from projectile to target nucleus is a unique feature of heavy-ion induced nuclear reactions that cannot be reproduced with light-ion beams. Much work has been done in studying multinucleon transfer above the Coulomb barrier with a variety of heavy-ion beams, targets, and experimental techniques.[1,2] Not only cross sections, but also product kinetic energies and angles of emission, have been determined in order to elucidate the details of transfer mechanisms. For example, Wolfgang and co-workers,[3-7] and more recently many others,[8-22] have taken advantage of radioactive-decay properties to measure these quantities for the heavy (and sometimes light) products of the reaction. In-beam experiments, often with ΔE-E counter telescopes, have distinguished by atomic number between the various light nuclei produced in transfers.[23-30] A refinement of this technique has used magnetic analysis in conjuction with counter telescopes to separate the transfer-reaction products according to atomic number and mass.[31-36] These investigations have served to delineate some of the properties that characterize transfer reactions, and have led to the development of theoretical calculations that attempt to predict such properties as kinetic energy and angular distributions, cross sections, dependence upon reaction Q values, etc.[5,6,17,20,21,26-28,34,37-44]

The heaviest target used in the above-referenced studies of heavy-ion transfer reactions was ^{232}Th. Extending such work to much heavier targets is difficult because of the small amounts of target material available, the special precautions required in handling such α-active material, and the small reaction cross sections encountered. Most of what has been done in this area has been limited only to excitation-function measurements and the question of the competition between fission and spallation in excited actinide nuclei.[45,46] Recently, Sikkeland *et al.*[47,48] have presented data and calculations for cross sections of complete-fusion and transfer reactions induced by heavy ions on heavy targets (for our purposes here, the terms complete-fusion and compound-nucleus reactions are synonymous). Many questions remain, however, about the mechanisms of transfer reactions, especially in the heavy-element region.

In this paper, we report on a comparative study of the reactions ^{239}Pu(^{12}C, αxn) and ^{238}U(^{12}C, yn) leading to the same observed radioactive products, ^{245}Cf and ^{244}Cf. The latter reactions have been

shown, in previous excitation-function measurements,[48] to proceed via compound-nucleus formation and decay; we have determined recoil properties for the U + C system to verify this conclusion, and then have used these results as standards for comparison and contrast with the data obtained for Pu + C. Absolute cross sections and recoil range and angular distributions have been measured to characterize these reactions (see Ref. 49 for a brief discussion of some relevant work), and to allow for comparison with model-dependent calculations.

Such data are pertinent to experiments designed to search for new elements and isotopes, since quantitative information of the competing processes that occur in the interactions of heavy ions with heavy elements may indicate which reactions are most favorable for producing a given nuclear species.[50] Detailed differences between complete- and incomplete-fusion reactions may, in some instances, also serve as aids in identifying the products of heavy-ion reactions.[51]

II. EXPERIMENTAL PROCEDURES

The experiments performed in this work were of two general types: (a) measurements of cross sections for the production of ^{245}Cf and ^{244}Cf in the nuclear interactions of heavy ions with actinide-element targets, especially the reactions of ^{12}C with ^{239}Pu and ^{238}U; and (b) measurements of range and angular distributions of ^{245}Cf and ^{244}Cf recoil nuclei from thin ^{238}U and ^{239}Pu targets. First we shall discuss experimental details common to both types of experiments, and then consider features that are specific to either experiments (a) or (b).

Targets were prepared in the form of the actinide oxides. Because most of the transfer studies were done with ^{239}Pu, extra care was taken to remove impurities from it: The final concentrations of Th, U, and Am were $\leq$ 100 ppm in the ^{239}Pu targets. The Pu contained 95% of mass 239, ~5% of 240, and < 1% of 241. The targets were prepared by electrodeposition of the actinide nitrates from isopropyl alcohol onto Be or Au foils, followed by conversion to the oxide by heating at $\gtrsim$ 500°C. Target thicknesses were always smaller than the ranges of the recoil nuclei, and were respectively 200 and 166 μg/cm^2 for the oxides of ^{238}U and ^{239}Pu.

Irradiations were performed at the Oak Ridge isochronous cyclotron (ORIC). Although most of the experiments used ^{12}C as the projectile, beams of ^{14}N and ^{16}O were also used. Because ORIC is a variable-energy cyclotron, beams at several different energies were extracted for direct irradiation of the targets. When necessary, a thin (2.5 mg/cm^2) Be absorber was used to reduce the beam energy; the total energy loss in the degrader and target-backing foils never exceeded 15 MeV and was usually < 10 MeV. The energy of the extracted beam was accurately measured with an analyzing magnet prior to each irradiation.

The nuclides ^{245}Cf and ^{244}Cf were selected for these experiments because their α-decay branches are large, and their half-lives are convenient both for absolute cross-section determinations ($\lesssim$ 1 h) and for recoil measurements ($\gtrsim$ 10 min). Also, the Cf radioactivities were about the only heavy elements observed in the recoil experiments so that the measured α-particle spectra, in the range of 6.5 to 8.5 MeV, were relatively simple to interpret. Details of the decay properties[52–54] of these two nuclides are given in Table I, along with data for other Cf, Es, and Fm isotopes that could be produced in the Pu + C reactions. α-particle spectra were taken as a function of time so that both the characteristic α-particle energies and half-lives could be used to identify ^{245}Cf and ^{244}Cf. The decay data were then analyzed with a least-squares procedure.

A. Excitation functions

Measurements of the excitation functions were done with a gas-jet system that has previously been described in detail.[55] The system is characterized by the automatic collection of radioactive products during irradiation, followed by the measurement of α spectra as a function of time. Such parameters as irradiation time, counting interval, and the number of spectra to be recorded can be

TABLE I. Decay characteristics of Cf, Es, and Fm nuclides (Refs. 52–54).

Nuclide	Half-life	E_α (MeV)	α/Total
^{246}Cf	36 h	6.76	0.78
		6.72	0.22
^{245}Cf	44 min	7.12	0.30
^{244}Cf	19.4 min	7.21	0.75
		7.17	0.25
^{243}Cf	10.3 min	7.05	~0.10
^{246}Es	7.3 min	7.33	0.10
^{245}Es	1.3 min	7.70	0.17
^{244}Es	40 s (EC)	...	...
^{249}Fm	~2.5 min	7.53	...
^{248}Fm	38 s	7.87	0.80
		7.83	0.20
^{247}Fm	35 s	7.93	~0.3
		7.87	~0.7
	9.2 s	8.18	...
^{246}Fm	1.2 s	8.24	0.92
^{245}Fm	4.2 s	8.15	...
^{244}Fm	3.3 ms (SF)	...	...

programmed prior to the start of the experiment; the sequence of irradiation and counting period is then automatically repeated until sufficient counting statistics are accumulated.

Because the over-all efficiency of the gas-jet system was not accurately known, additional experiments were done with radiochemical techniques to measure absolute cross sections and to serve as a scale normalization for the gas-jet results. Targets of ^{238}U and ^{239}Pu were prepared on Au foils that were thicker than the recoil ranges so no product nuclei would be lost. The chemical separation scheme for the irradiated targets used anion-exchange techniques for the clean, rapid (< 10 min) separation of the product Cf activities (in strong HCl solution) from the dissolved U or Pu targets and Au backing foils. Aliquots of a ^{252}Cf standard solution were used to determine the chemical yields of these procedures.

B. Recoil experiments

The recoil measurements were made in a scattering chamber, schematically illustrated in Fig. 1, to obtain information on the ranges and emission angles of the recoiling Cf nuclides. Because of the low cross sections encountered in this work, microamperes of beam were required on target. Mechanical collimation to define the position of the beam precisely could not be used because of the resulting low beam intensity. Instead, a 1-cm-diam collimator was used, and the beam was focused with quadrupole magnets to give a small spot on target, ~0.4 cm in diameter.

For the range distributions, a stack of thin carbon foils (each foil was 20 or 40 μg/cm^2 thick) was placed downstream from the target. A collimator between target and catchers ensured that the same solid angle was subtended by each catcher in the stack; the angular interval covered from 0° to 10.7° with respect to the beam. For the angular distributions, thick (~9 mg/cm^2) aluminum catcher foils were placed on an equatorial strip around the target. The catchers subtended intervals of either 3° or 5°, with θ varying from 4° to 45° in the lab system. This arrangement directly gave angular distributions that were proportional to $d\sigma/d\Omega$ rather than to $d\sigma/d\theta$.

After each irradiation, the catcher foils were manually removed from the scattering chamber, and assayed for α-particle activity. The counting system contained four Si(Au) detectors which were operated independently and communicated, via a multiplexer, with a multidimensional analyzer. Thus, α spectra from four catcher foils could be simultaneously recorded during the same counting period.

III. RESULTS AND DISCUSSION

A. Cross sections

Preliminary experiments were performed with the gas-jet system to compare the yields of ^{245}Cf and ^{244}Cf produced in the reactions, ^{239}Pu(^{12}C, αxn), ^{235}U(^{16}O, αxn), ^{237}Np(^{14}N, αxn), ^{242}Pu[^{12}C, $\alpha(x+3)n$], and ^{238}U(^{12}C, yn). Because of the low yields found for some of these reactions, one can only make some qualitative statements about the various (heavy-ion, αxn) reactions: (a) the yields (identified by the targets used) followed the trend ^{239}Pu > ^{235}U > ^{237}Np and (b) ^{239}Pu > ^{242}Pu. Result (a) is taken as evidence that the probability of transfer decreases as the "size" or atomic number of the transferred aggregate increases. Since these reactions presumably involve separation of the projectile into an α particle and other residue (see discussion below of recoil data), it is reasonable that larger yields are observed for α-cluster nuclei such as ^{12}C and ^{16}O than with ^{14}N. Result (b) shows that $\sigma(^{12}\text{C}, \alpha xn)$ is larger for $x = 2$ or 3 than for $x = 5$ or 6, and indicates that

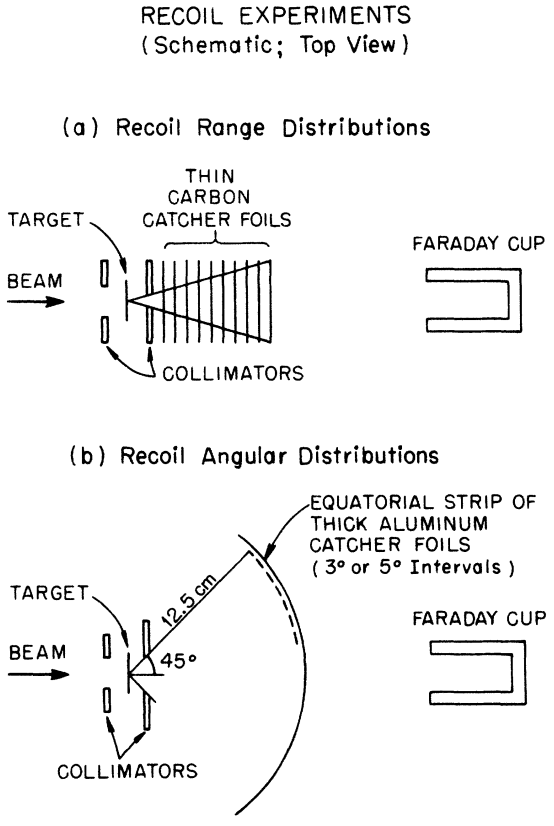

FIG. 1. Schematic illustration of apparatus used in determining range and angular distributions of recoil nuclei. The range distributions were measured over the angular interval, $0 \leq \theta \leq 10.7°$.

fission effectively competes with the evaporation of more than two or three neutrons.

Based on these results, we concentrated our efforts on a comparison of the ^{239}Pu(^{12}C, $\alpha 2n$ and $\alpha 3n$) reactions with the ^{238}U(^{12}C, $5n$ and $6n$) reactions, which had been shown previously to proceed via compound-nucleus formation and decay.[48] Absolute cross-section measurements of the ^{238}U + ^{12}C reaction were made at three energies and found to be in reasonably good agreement with published results.[48] Our excitation-function data for ^{239}Pu + ^{12}C are shown in Fig. 2. The solid lines connect the measured values for ^{245}Cf and ^{244}Cf, while the dashed curves are the results of theoretical calculations. Some evidence was obtained, with poor statistics, that ^{246}Cf is also produced in these reactions. The experimental points were determined with the gas-jet system, and normalized to absolute radiochemical measurements for ^{245}Cf at 63 and 70 MeV; because the radiochemical procedures took some 50 min to complete, little or no ^{244}Cf was seen. The contribution to the ^{245}Cf yield from the reaction ^{239}Pu(^{12}C, $2n$)^{249}Fm followed by α decay is expected to be negligible, as indicated by the calculated curves in Fig. 2, because of the inhibiting effect of the Coulomb barrier in the heavy-element region.

We can conclude from several arguments that the contributions to the observed Cf activities from radioactive decay of other Fm or Es nuclides (Table I), produced in either (^{12}C, xn) or (^{12}C, pxn) reactions, are also negligible. For example, for the Fm nuclei, the measured range and angular distributions for ^{245,244}Cf (to be discussed below) are not characteristic of compound-nucleus reactions, as would be the case if (^{12}C, xn) reactions were involved. Also, data for ^{239}Pu(^{12}C, xn) and similar reactions,[56,57] and the calculations in Fig. 2, indicate values of $\lesssim 1$ μb for ^{248}Fm and ^{247}Fm, much smaller than the cross sections determined for ^{245}Cf and ^{244}Cf. And although ^{246}Es and ^{245}Es have α-decay branches and half-lives that are appropriate for detection with the gas-jet system, no α peaks of Es nuclides were seen in the spectra. The Cf data thus should be representative of (^{12}C, αxn) reactions only.

The calculations shown in Fig. 2 were performed with computer programs developed by Sikkeland and colleagues[47,58] to treat heavy-ion (HI) reactions on actinide elements. Because the theory has been amply discussed in the literature (see Refs. 47 and 58 and bibliographies therein), we shall just outline the principles of the calculations. For the (HI, xn) reactions, one (a) assumes compound-nucleus formation and decay, (b) calculates the total reaction cross section with an optical potential, (c) uses the sharp cutoff model to calculate the compound-nucleus formation cross section as a function of angular momentum, (d) neglects charged-particle evaporation (see Ref. 59 for a discussion of the validity of this assumption) and uses the Jackson model to calculate probabilities of neutron evaporation, and (e) includes fission-evaporation competition by using semiempirical values of Γ_n/Γ_f that do not depend on angular momentum or excitation energy.

Recently, Sikkeland, Shafrir, and Trautmann[47] have extended these calculations to include transfer reactions, such as (^{12}C, αxn). Values computed with their code are shown for the Cf nuclides in Fig. 2. The rationale of the calculations follows that described above, with the following modifications: (a) The total cross section for transfer reactions is gotten from those angular-momentum waves above the sharp cutoff value; (b) the reaction is assumed to proceed in a two-step sequence in which the transfer of part of the projectile to the target nuclues occurs in the first step; (c) the probability for a given transfer is obtained from trends empirically determined for a variety of transfer reactions; (d) the second step of the reaction involves the customary deexcitation of the residual nucleus by neutron evaporation and fission; (e) no fission is assumed to occur during the first step of the reaction. For example, for the cases shown in Fig. 2, one assumes that ^{245}Cf

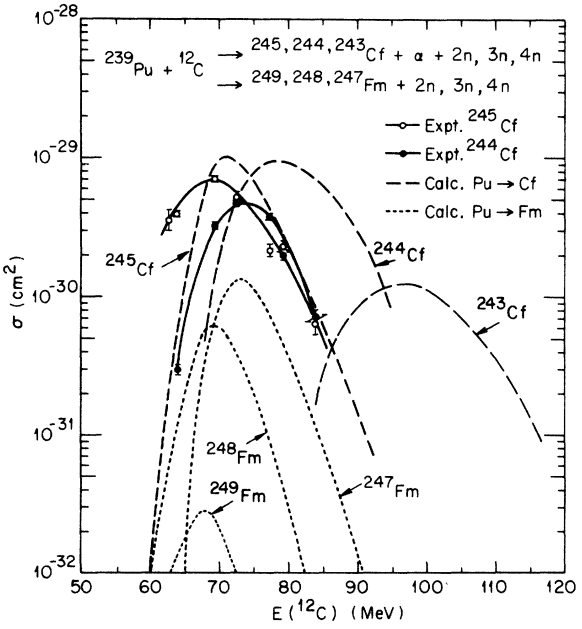

FIG. 2. Excitation functions for the reactions ^{239}Pu + ^{12}C. The solid curves connect the data points measured for ^{245}Cf and ^{244}Cf, while the broken curves are calculations of (^{12}C, yn)Fm and (^{12}C, αxn)Cf reaction cross sections, done with the programs of Sikkeland *et al.* (Refs. 47 and 58).

and ^{244}Cf arise from the transfer of ^{8}Be from ^{12}C to ^{239}Pu, forming excited ^{247}Cf, which then emits two or three neutrons to produce the observed nuclides.

It is seen that the transfer calculations do succeed in approximately reproducing the magnitudes and energy dependence of the observed cross sections. Considering the many assumptions and approximations in the calculations, this agreement is considered encouraging. (Additional support for such a description of transfer reactions comes from the recoil data to be discussed below.) The data and calculations indicate that over the range of interest $\sigma(C, \alpha 2n\text{-}\alpha 3n) >> \sigma(C, 2n\text{-}4n)$, a result that is due mainly to the known dependence of Γ_n/Γ_f on Z and N. For although the computed probability of formation of compound-nucleus ^{251}Fm is much larger than that of transfer product ^{247}Cf, the deexcitation by fission is much more likely for the Fm's, so that the final calculated Cf cross sections are larger than those for the Fm isotopes.

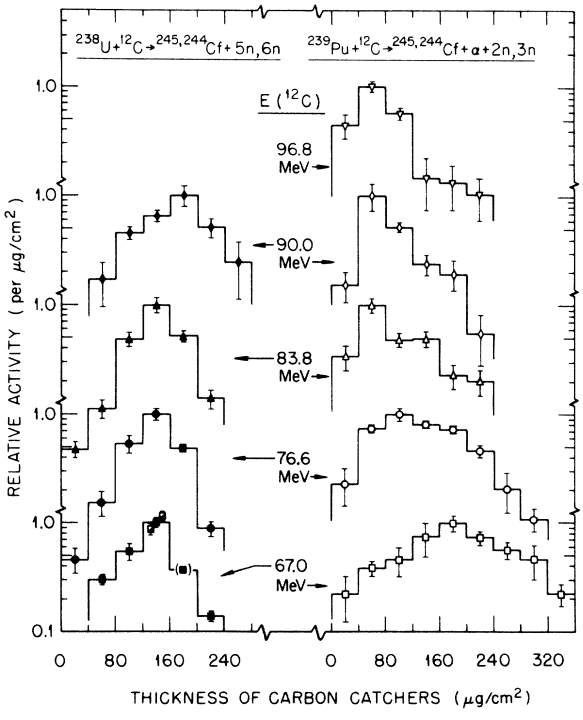

FIG. 3. Range distributions of ^{245}Cf and ^{244}Cf from the reactions ^{238}U + ^{12}C and ^{239}Pu + ^{12}C. The data points are the relative activities observed in each carbon catcher; no correction has been applied for stopping in the targets. The values shown are for carbon foils of 40 μg/cm^2, except for the two points (half-closed squares) for ^{238}U + 67 MeV ^{12}C, where foils of 20 μg/cm^2 were used. See text and Fig. 5.

B. Recoil measurements

The distributions in range and in angle of the Cf recoils are shown, respectively, in Figs. 3 and 4. Because of the energy spread of the observed α peaks resulting from the thickness of the targets and of the catcher foils, and because of the generally low counting rates observed, it was not possible to separate accurately the results for ^{245}Cf and ^{244}Cf. Instead, at each bombarding energy, the best average half-life resulting from the mixture of the two Cf activities in all of the catcher foils was determined by the least-squares method and then used to fit the counting data for each individual foil making up the distribution. As expected from the excitation functions of Fig. 2, at lower bombarding energies, the average half-life was close to 44 min, that for ^{245}Cf; as the energy increased, the average half-life became progressively smaller, finally attaining a value close to 19 min, that of ^{244}Cf. This use of average half-life to give one (average) distribution for both Cf's at each energy assumes that the separate distributions for ^{245}Cf and ^{244}Cf are very similar, as would be expected if the two nuclides, differing

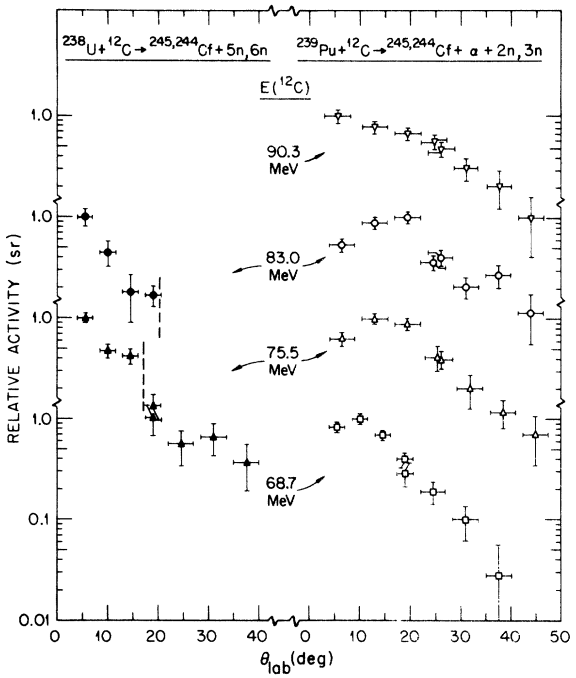

FIG. 4. Relative angular distributions of ^{245}Cf and ^{244}Cf from the reactions ^{238}U + ^{12}C and ^{239}Pu + ^{12}C. The distributions are proportional to $d\sigma/d\Omega$. For the ^{238}U + ^{12}C reactions, the dashed vertical lines represent the maximum angles in the laboratory system at which the Cf products should be observed, as calculated from reaction kinematics.

in mass by only one neutron, were produced by essentially the same mechanism. If this assumption were not true, i.e., if the separate distributions were grossly different, the observed average half-life should have changed from foil to foil within a given distribution measurement as the relative amounts of the two Cf isotopes changed. This change was not observed.

The data points in Fig. 3 result from replicate measurements made with 40 $\mu g/cm^2$ carbon foils, except for the two half-shaded squares for ^{238}U +67 MeV ^{12}C, which were done with 20 $\mu g/cm^2$ catchers. The point enclosed in parentheses at 67 MeV is only an estimate, based on the general shapes of the U+C distributions. Nominal uncertainties in the thicknesses of the carbon foils were ±10%. No correction has been applied in Fig. 3 for energy loss of the recoils in the targets (see below, where such corrections are included in Fig. 5). It is quite clear from Fig. 3 that the range distributions for $^{245,244}Cf$ differ markedly for the two targets studied. The distributions for $^{238}U + ^{12}C$ are fairly symmetric, with a most probable value that increases with increasing bombarding energy, while the $^{239}Pu + ^{12}C$ distributions are asymmetric, extending to large range values, but with peak values that decrease with increasing energy.

Figure 4 shows the measured angular distributions, where the data points are again averages of replicate measurements. Since measurements were made at only four angles during any given irradiation, the entire distribution had to be constructed from several irradiations at the same energy. The two closely positioned points shown for almost every distribution at ~20° or ~25° demonstrate the degree of consistency in matching up the different parts of a given distribution. As with the range distributions, the data of Fig. 4 show definite differences for the two systems studied. The U+C data are forward peaked, and drop off rapidly with increasing angle, reaching ~15% of the maximum value before ~20°. For Pu+C, the distributions are much broader. Even at 68.7 MeV, where the distribution is most forward peaked, the value of ~15% of the maximum occurs at ~27°. Most noticeable about the angular distributions at 75.5 and 83.0 MeV is the existence of a peak at ~17°. Similar peak values have been measured in transfer reactions induced by ^{12}C on Bi and Au, where they were interpreted as being due to transfer of ^{8}Be from ^{12}C to the target nucleus.[13]

The angular distribution for Pu+C at 90.3 MeV is of interest because, although it is still rather broad, its maximum value has changed from ~17° to a much more forward angle, $\lesssim 5°$. We observed a similar forward-peaked distribution, not shown in the figure, at 96.5 MeV, but with poorer counting statistics. One might consider such behavior to be characteristic of a contribution from compound-nucleus reactions, either with the Pu nuclei or with the Pb impurity in the target. Indeed, α spectra from the gas-jet experiments at the higher bombarding energies do show several peaks that are apparently related to Ra activities produced from Pb(^{12}C, xn) reactions. However, those nuclides in the Pb-Ra region of the Periodic Table that emit α particles ~7.1 MeV have half-lives of a few seconds or less, far shorter than that of ^{244}Cf. More importantly, the average recoil ranges measured at $\gtrsim 90$ MeV (see discussion below concerning Fig. 5) are much lower than the expected complete-fusion values for either Pu+C or Pb+C, so that compound-nucleus reactions do not seem to be important contributors to the data.

The forward-peaked angular distributions may be associated with production of ^{243}Cf, which becomes significant above ~90 MeV. Yet if complete-fusion reactions are discounted, one cannot explain the drastic change in angular distributions by the presence of ^{243}Cf; a change in mass from 244 to 243 should not grossly affect the outcome of a transfer reaction. The behavior observed at $\gtrsim 90$ MeV may thus signify a change in the mechanism of the transfer reactions leading to the Cf nuclides (see Sec. III D).

The finite thickness of the targets affected the distributions of Figs. 3 and 4 in several ways. First, the ratio of recoil range to target thickness, R/W, determines the fraction of activity that escapes from the target, and so can affect the observed counting rates and cross sections. However, using expressions developed by Alexander,[1] we found that for the worst case encountered in this work, i.e., for the lowest value of $R/W = 1.7$, the fraction of activity remaining in the target was 0.4%, a negligible amount.

Slowing down in the target lowers the average recoil range measured in the carbon catchers, and must be taken into account; it also broadens the observed distributions. This straggling effect is seen to be small in the U+C data of Fig. 4. Here the vertical dashed lines indicate the maximum angles at which heavy recoil nuclei should be observed in the laboratory system, an effect arising from reaction kinematics when the velocity of the center of mass system (c.m.s.) in the laboratory frame is greater than the velocity of the recoil nucleus in the c.m.s. For the 75.5 MeV data, counts are indeed seen beyond the calculated maximum angle (for the 83 MeV run, no points were measured beyond 20°). Integrating over the angular distribution at 75.5 MeV indicates, how-

ever, that ~90% of the observed activity is found at angles less than the maximum angle, so that straggling does not grossly distort the observed U+C distributions. Similar calculations for the Pu+C reactions give maximum angles that vary from 30° at 69 MeV to 34° at 90 MeV. It is seen that the relative activity observed beyond these angles is quite small.

Uncertainties in the range and angular distributions caused by the finite size of the beam spot are also small. Estimates of the solid angles subtended by the various foils in the catcher stack are the same as for a point beam. And the resultant maximum spread in the angular interval per catcher used in the angular-distribution determinations is estimated to be 0.9°, much smaller than the angular widths of the foils themselves.

Plotting the fractional cumulative activity on probability paper as a function of total catcher thickness demonstrates that the range distributions from U+C are Gaussian, as is expected for compound-nuclear processes.[1] From such plots, one can extract average ranges and total straggling parameters, ρ. These values of $\rho \approx 0.3$ are consistent with values found in other (HI, xn) reactions (see, e.g., Ref. 60); we have not attempted, however, to use these values to extract specific straggling parameters for the nuclear-velocity distribution and the stopping process.

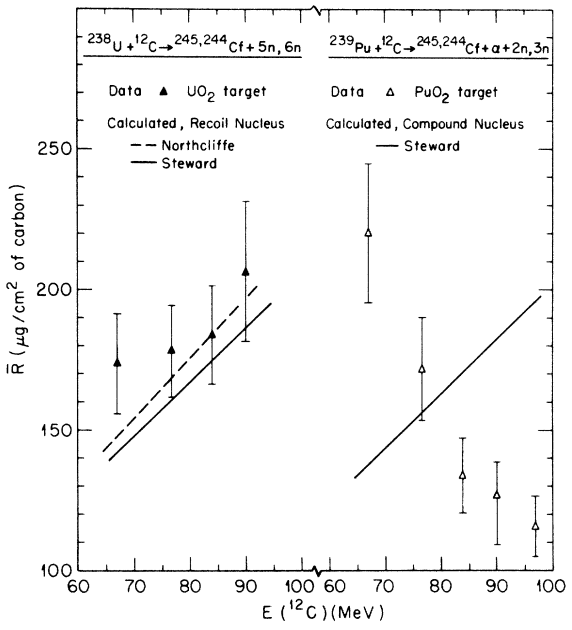

FIG. 5. Average ranges, $\bar{R}$, in carbon (over the angular interval from 0 to 10.7°) of the recoil nuclei ^{245}Cf and ^{244}Cf from the reactions $^{238}U + ^{12}C$ and $^{239}Pu + ^{12}C$. Each data point has been obtained from the corresponding range distribution shown in Fig. 3, and appropriately corrected for stopping in the targets. The lines are ranges calculated by assuming full-momentum transfer in the reactions, and using the range-energy relations of either Steward (Ref. 61) or Northcliffe and Schilling (Ref. 62). See text for details.

The average recoil ranges, $\bar{R}$, equal to the centroids of the range distribution of Fig. 3 for the angular interval 0 to 10.7°, and subsequently corrected for stopping in the targets, are shown in Fig. 5. The recoil energies E_R corresponding to these experimental values were evaluated with the range-energy program of Steward,[61] and are listed in Table II. Because $\cos\theta \simeq 1$ over the angular interval covered, it was not necessary to correct the range values for the fact that many of the recoils did not enter the catcher at normal incidence. In Fig. 5, errors on the points, ~10%, were derived by propagating the uncertainties in activities and catcher thicknesses for each of the respective distributions. Corrections for the effect of energy loss of the recoils in the targets were evaluated with the expressions

$$\Delta R_C = (S_T/S_C)W/2 ,$$

$$\bar{R} = R_C + \Delta R_C ,$$

where S_T and S_C are the stopping powers taken from Steward[61] for the target and carbon catcher, respectively, at each recoil energy; W is target thickness; ΔR_C is the reduction in range, in terms of the carbon catchers, due to slowing down in the targets; and R_C is the measured (uncorrected) average range in carbon (from Fig. 3). For the thin targets used, all of the recoils were assumed to originate at the midpoint of the target; S_T was evaluated for the oxide form of each target. The corrections ΔR_C are appreciable, the largest being ~30% of $\bar{R}$ at the lowest recoil energies encountered. Furthermore, the ΔR_C values depend upon calculated stopping powers that may differ from one compilation to another. These *caveats* should be remembered when considering the *absolute* magnitudes of $\bar{R}$.

TABLE II. Average recoil energies E_R of Cf nuclides.

$E(^{12}C)$ (MeV)	E_R (MeV)[a] $^{238}U(^{12}C, 5n\text{-}6n)$	$^{239}Pu(^{12}C, \alpha 2n\text{-}\alpha 3n)$
67.0	4.0 ± 0.4	5.2 ± 0.7
76.6	4.1 ± 0.4	3.9 ± 0.5
83.8	4.2 ± 0.4	3.0 ± 0.4
90.0	4.8 ± 0.5	2.9 ± 0.4
96.8		2.6 ± 0.3

[a] Evaluated from experimental $\bar{R}$ values of Fig. 5 and the range-energy values of Steward (Ref. 61).

Nevertheless, the strikingly different trends exhibited by the U + C and Pu + C data are significant, because the energy dependence of the $\bar{R}$ values in Fig. 5 does not depend upon the exact values of ΔR_C. That is, the ratio S_T/S_C was found to be essentially constant for all recoil energies considered, so that the values of ΔR_C did not change by more than ~2% for bombarding energies from 67 to 97 MeV.

In the next section, we shall discuss some models that can approximately account for the Pu + C data; first, the U + C data will be compared with ranges calculated with the assumption that the (C, *xn*) reactions proceed through compound-nuclear channels.

One of the traits thought to be specific for compound-nuclear reactions is complete transfer of the projectile's momentum to the compound system. The kinetic energy of the compound nucleus is

$$E_{CN} = E_P M_P / M_{CN} , \quad (1)$$

where E and M are energy and mass, respectively, and subscripts P and CN refer to projectile and compound nucleus. If one assumes that the velocity of the product recoil nucleus with mass M_R is equal to that of the compound nucleus, or equivalently, that the nuclear velocity is imperceptibly affected by the evaporation of neutrons, the recoil energy of the observed nucleus is

$$E_R = E_P M_P M_R / M_{CN}^2 . \quad (2)$$

Values of E_R were calculated with Eq. (2) for the system $^{238}U + {}^{12}C \rightarrow {}^{245}Cf$ and then expressed as ranges, using the tables of either Steward[61] or Northcliffe and Schilling.[62] These ranges were subsequently corrected for the effect of neutron evaporation; that is, the expected ranges, obtained from Eq. (2), were multiplied by the factor[60] $[1 + (2/3)(\bar{V}_R/v_{CN})^2]$. Here $\bar{V}_R$ is the average c.m.s. velocity imparted to the product nucleus by neutron emission, v_{CN} is the velocity of the compound nucleus in the laboratory system, and

$$(\bar{V}_R/v_{CN})^2 = [(E_P M_T/M_{CN}) + Q](M_{CN}^2/M_R^2 M_P E_P) , \quad (3)$$

where M_T is the target mass, and the Q value is that for formation of the compound system. These range corrections were small, varying from 1–2%. Because of differences in the ways in which electronic and nuclear stopping are treated in Refs. 61 and 62, two calculated range vs energy lines are drawn in Fig. 5. The agreement between theory and experiment is good, although the insufficient precision of the measurements, and uncertainties in ΔR_C, preclude detailed tests of range-energy theory as used in the cited references.

For $^{239}Pu + {}^{12}C$, the kinetic energies of the compound nucleus were calculated with Eq. (1), converted to ranges using Steward's treatment,[61] and drawn in Fig. 5. Although no corrections have been made here for evaporation of α particles or neutrons, the trend of increasing range with increasing bombarding energy, so characteristic of complete-fusion reactions, does not agree with the data for ^{245}Cf and ^{244}Cf from the reactions Pu + C. For example, the measured recoil range at 67 MeV is 1.6 times the expected complete-fusion (CF) value for Pu + C and decreases to 0.6 of the CF value at 97 MeV.

C. Kinematic model of transfer reactions

Recently, Bimbot and co-workers have analyzed the results of several transfer-reaction studies[13,15] by using reaction kinematics to indicate which reactions were most likely to contribute to the observed yields. Their method is general in that it only requires conservation of energy and momentum; it contains no assumptions about the details of the mechanisms involved in the transfer process.

To discuss the present recoil data for $^{239}Pu + {}^{12}C$, we will primarily make use of a more detailed semiclassical model, first presented by Strudler,[5,6] and more recently discussed by Williams[17] and by Hubert.[20,21] The main features of the model may be discussed with the aid of the vector diagram (in the laboratory system) in Fig. 6. The final velocity $\vec{V}_{Rf}$ at angle θ_R of the

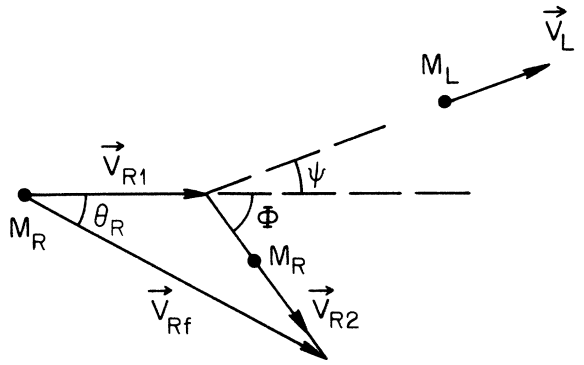

FIG. 6. Velocity diagram *in the laboratory system* of the two-step transfer model used in this work. Nucleus R (mass M_R) has an observed velocity $\vec{V}_{Rf}$ at angle θ_R that is the resultant of velocity $\vec{V}_{R1}$ at 0°, due to the transfer of some nucleons from projectile to target, and of velocity $\vec{V}_{R2}$ at angle Φ, due to Rutherford scattering with the remaining light particle L, with mass M_L.

heavy product of a transfer reaction is assumed to be the resultant of two processes in which: (1) An aggregate transfers from the projectile to the target nucleus, forming recoil nucleus R with velocity $\vec{V}_{R1}$, while (2) Rutherford scattering between nucleus R and the remaining light residue gives rise to velocity $\vec{V}_{R2}$ at angle Φ.

In detail, one finds for a transfer reaction denoted

$$P+T \rightarrow (T+A)+L \equiv R+L \ ,$$

where P, T, A, L, and R refer, respectively, to the projectile, target, transferred aggregate, light residue, and recoil nucleus, that for process (1)

$$\vec{V}_{R1}=(M_A/M_R)\vec{V}_P \ , \tag{4}$$

and for process (2)

$$\vec{V}_{R2}=[2M_L/(M_R+M_L)]\vec{V}_P\cos\Phi \tag{5}$$

with

$$\cos\Phi = B/(2E_0 - B) \ . \tag{6}$$

Here B is the Coulomb barrier for the interaction of the product nuclei R and L, at the minimum (touching) distance of closest approach D (with radius parameter r_0);

$$B = Z_R Z_L e^2/D \ , \tag{7}$$

$$D = r_0(M_R{}^{1/3}+M_L{}^{1/3}) \ , \tag{8}$$

and E_0 is the corresponding energy in the center of mass system,

$$E_0 = E_P[M_L M_R/M_P(M_R+M_L)] \ . \tag{9}$$

Implicit in process (1) is the notion of the transfer occurring at the nuclear surface. Eq. (4) is equivalent to the result obtained, for the case where nucleons transfer only from projectile to target, from the general treatment of transfer reactions given recently by Siemens *et al.*[41] and others.[42-44] The main results of process (1) are that the velocities of the projectile and the transferred agregate are equal, and that the system's motion is directed along 0°: Eq. (4) thus includes in the calculation recoil effects caused by the transfer of mass and momentum from projectile to target. However, Rutherford scattering, process (2), also has a considerable effect in the present model upon the final energy and angle of the heavy nucleus. We should add that the model treats only the kinematics of the reaction. It does not consider the details of the separation of the projectile into transferred aggregate and residual particle, nor the probability that a specific transfer process occurs.

The evaluation of $\vec{V}_{Rf}$ from Eqs. (4) to (9) is straightforward, and has been presented in detail

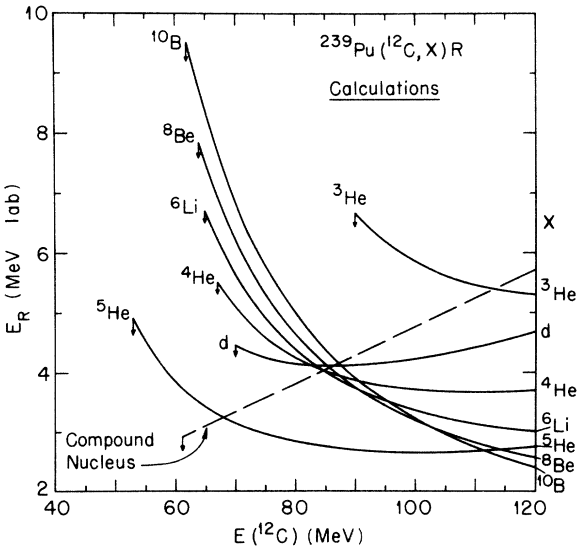

FIG. 7. Kinetic energies as a function of bombarding energy of the recoil nucleus R arising from the transfer reaction ^{239}Pu(^{12}C, X), as calculated with the two-step model described in the text. Curves are identified by the different emitted light particles X (the transferred aggregate is given by ^{12}C-X, and $R = {}^{239}$Pu + ^{12}C-X). The vertical arrows show the cutoffs imposed by the Coulomb barrier. The dashed line gives the kinetic energy of the compound nucleus ^{239}Pu + ^{12}C.

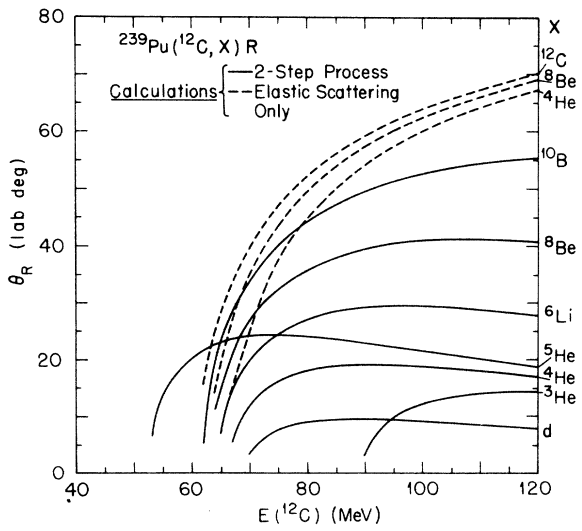

FIG. 8. Angle of emission of recoil nucleus R for the transfer reaction ^{239}Pu(^{12}C, X), associated with each value of E_R shown in Fig. 7. See the caption of Fig. 7 for details. Solid curves are for the two-step process, while the dashed curves show only the effect of the elastic scattering between particle X and nucleus R.

recently.[17,20] Required for the calculations are the masses and atomic numbers pertinent for any assumed transfer path [such as ^{239}Pu(^{12}C, X)R, where X is the light residue, ^{239}Pu + ^{12}C-X = R is the corresponding heavy recoil nucleus, and (^{12}C-X) is the transferred aggregate], the kinetic energy E_p of the projectile, and r_0, which is the only adjustable parameter in the calculation. The computations then give a final recoil energy E_R at a specific lab angle θ_R for nucleus R. No distributions in energy or angle are derived from this model, so the predictions must be compared with the centroids of the measured distributions. Note also that the model deals only with the transfer process; we neglect the small effects in the final recoil energies and angles due to the neutron evaporation that follows the transfer reaction (charged-particle evaporation is negligible for heavy-element targets). Hence, the results calculated for the assumed transfer paths, ^{239}Pu(^{12}C, ^{3}He)^{248}Cf, (^{12}C, ^{4}He)^{247}Cf, and (^{12}C, ^{5}He)-^{246}Cf are all to be directly compared with the data for ^{239}Pu + ^{12}C → ^{245,244}Cf (the role of neutron evaporation will be important in discussing excitation energies in Sec. III E).

To illustrate the results obtainable with this model, we show in Figs. 7 and 8 calculated values for a variety of reaction paths ^{239}Pu(^{12}C, X)R; the various curves are identified by the light partner X in the reaction. The recoil energies vs bombarding energy for several transfer reactions are presented in Fig. 7, as well as that expected for the compound-nucleus (CN). The curves for the transfer reactions are seen to be quite different than the CN line, giving much lower recoil energies than that expected for the complete-fusion reaction at high bombarding energies, and significantly higher recoil energies than the CN at energies near the Coulomb barrier (vertical arrows, ↓, on the curves denote the lower limits imposed in the calculations by the Coulomb barrier). These trends are qualitatively in agreement with the data shown in Fig. 5.

Two general types of behavior are seen in Fig. 7. The first of these is for transfers in which the ratio of mass to atomic number, M/Z, in particle X is equal to that of the projectile, as exemplified by d, ^{4}He, ^{6}Li, ^{8}Be, and ^{10}B: Near the Coulomb barrier, elastic scattering, process (2), predominates, so that E_R depends mainly on Z and M of particle X; the values of E_R follow the sequence ^{10}B > ^{8}Be > ^{6}Li > ^{4}He > d. As the projectile energy is increased, process (1), which depends on the mass of the transferred aggregate, becomes more important. The above sequence of E_R values is reversed (causing the curves to cross each other) since (^{12}C-X) is smallest when X is largest. The second type of behavior is noted for transfers in which Z of particle X is kept constant and M changes, as for ^{3}He, ^{4}He, and ^{5}He: The curves have similar shapes and do not intersect. Process (1) is important so that the lightest particle X (here ^{3}He), or heaviest transferred cluster (^{9}Be), gives the highest E_R values; the cutoff energies, however, are rather different for the different He isotopes. The curves giving the values of θ_R that correspond to each E_R value of Fig. 7 are shown in Fig. 8 for the two-step transfer model (solid curves). At energies well above the Coulomb barrier, θ_R tends to be approximately constant, but decreases rapidly in the vicinity of the barrier. Such behavior is also qualitatively in accord with our data (Fig. 4). It is seen that θ_R in general increases with increasing M and Z of particle X.

The effects of the second step, or process (2) (i.e., of elastic scattering only), on θ_R are shown as the dashed curves in Fig. 8. The curve labeled ^{12}C is for elastic scattering of the projectile and ^{239}Pu target, while the other two curves are for the elastic scattering of particle X and nucleus R that were formed in process (1), i.e., for scattering of ^{8}Be from ^{243}Cm and of ^{4}He from ^{247}Cf. Clearly, the curves for elastic scattering of ^{8}Be and ^{4}He are very different from the curves (solid) derived from the two-step model for these same particles, especially at the higher energies.

The differences between the solid and dashed curves in Fig. 8 reflect effects due to process (1), namely the transfer of momentum in the forward direction accompanying the transfer from projectile to target nucleus. We stress this point because the two-step model predicts that θ_R will be much smaller than the grazing angle (the dashed curves for elastic scattering) when the number of transferred nucleons is appreciable. This question is significant because Toepffer[40] has derived an expression for the optimal Q value (or equivalently, excitation energy) for transfer reactions based on the assumption that the optimal scattering angle for transfer reactions is always the grazing angle.

D. Comparison with recoil data

The data for the reactions ^{239}Pu(^{12}C, αxn)-^{245,244}Cf are compared with the model-dependent calculations in Fig. 9. It should be remembered that the ranges of Figs. 3 and 5 were measured only over the angular interval 0 to 10.7°, whereas the angular distributions show a maximum at ~17°. The calculated E_R values, which correspond to the maxima of the angular distributions, thus may not be exactly equivalent to the experimental

values, but should hopefully display a similar dependence on bombarding energy, as in indeed seen in Fig. 9.

The θ_R values are taken from the angular distributions of Fig. 4. The circles (●) give the centroids of the distributions, and the triangles (▲), the angles at which the maxima of the distributions occur; for the centroids, the error bars were obtained by propagating the errors on the separate components of the respective angular distributions; the uncertainties, not shown, on the maxima (▲) are taken to be at most $\pm\frac{1}{2}$ of the angular spread covered by the catcher foils (Fig. 4), i.e., either ±1.5° or ±2.5°.

The curves in part (a) of Fig. 9 were calculated with the two-step model described above for the transfer of a Be cluster from the ^{12}C projectile to the target (labels on the curves are for particle X remaining after the transfer). An $r_0 = 1.65$ fm was used in the calculations, in agreement with

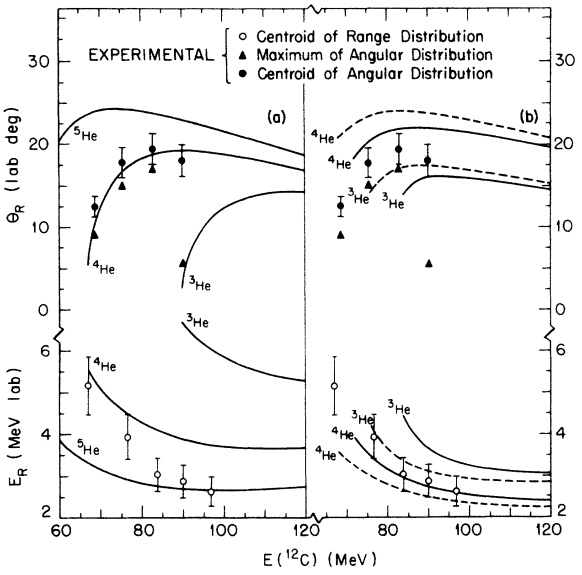

FIG. 9. Results derived from the range and angular distributions measured for ^{245}Cf and ^{244}Cf (from ^{239}Pu $+^{12}$C), compared with calculations based on two different kinematic models in (a) and (b). The experimental recoil energies E_R, listed in Table II, were obtained from the range values of Fig. 5 and Steward's range-energy values (Ref. 61). Lab angles θ_R were gotten from the distributions of Fig. 6: The circles represent the centroids and the triangles, the maxima, of the angular distributions. Part (a) shows calculations with the two-step model, and (b) with a model involving only Rutherford scattering. The curves are identified by the helium nuclide remaining after the transfer. In part (b), the dashed curves are for the cases where sufficient excitation energy remains in the respective intermediate nucleus to evaporate neutrons and reach ^{245}Cf; the solid curves, to reach ^{244}Cf. See text.

r_0 values found in other transfer studies, e.g., Refs. 21 and 26.

The possibility that the observed Cf activities could arise from radioactive decay of either Fm or Es nuclides was ruled out in Sec. III A. This conclusion is supported by the recoil data of Figs. 3–5 and 9, which clearly show that compound-nucleus decay is not involved in these reactions. Also, the calculated curves for the deuteron in Figs. 7 and 8 are quite different from the data shown in Fig. 9. Thus, the recoil data for the Cf's are thought to be representative of (^{12}C, He)-type transfers, with no corrections required for contributions from (^{12}C, xn) or (^{12}C, pxn) reactions.

The agreement between the calculations and data in Fig. 9(a) is reasonable for both E_R and θ_R. In particular, the model predicts a most probable value of ~18° for θ_R at higher energies, in accord with the present results and with data reported by Bimbot, Gardes, and Rivet[13] for other (^{12}C, αxn) reactions. It also reproduces the observed rapid decrease in angle with decreasing bombarding energy; forward peaking of this kind, near the barrier, had previously been ascribed solely to complete-fusion reactions followed by radioactive α decay.[13] The values of θ_R observed for multi-transfer reactions are much smaller than the classical grazing angle, as has been also noted in Refs. 15 and 35.

A comment about the observed maximum at ~5° in the angular distribution at 90.3 MeV is in order here. If, as discussed in Sec. III B, the abrupt change in peak angle from ~17 to ~5° is indeed associated with the Cf nuclides, it may support the proposal[63] that, at higher bombarding energies, the nuclear force appreciably perturbs the trajectories of products X and R, causing forward peaking of the angular distributions.

In evaluating the two-step transfer model, one should be mindful of the simple premises on which it is based, and that it neglects effects of, e.g., angular momentum and the reaction Q value upon E_R and θ_R. The model can be useful in deciding that certain transfers such as (C, p, or d) are much less likely than (C, He) in the reactions studied here. But it is probably unrealistic to expect the model to indicate the mass of the He isotope involved, i.e., to pinpoint a transfer involving ^{8}Be and ^{4}He rather than ^{7}Be and ^{5}He; a few such different reaction paths may in fact contribute to the data.

Another factor to consider is that this model is not unique. Other models of transfer reactions may lead to different conclusions so that one must be cautious in interpreting experimental results such as have been presented here. For example, a somewhat different model is compared with

the data in Fig. 9(b). Galin *et al.*[26-28] have performed calculations of few-nucleon transfers by assuming that the incoming and outgoing trajectories may be expressed solely in terms of Rutherford scattering. They require the transfer to occur at the point of closest approach $R_{\min}$, where the incoming (i) and outgoing (f) trajectories meet. Then

$$R_{\min} = \frac{Z_P Z_T e^2}{2\bar{E}_i}\left(1+\csc\tfrac{1}{2}\theta_i\right) = \frac{Z_L Z_R e^2}{2\bar{E}_f}\left(1+\csc\tfrac{1}{2}\theta_f\right), \quad (10)$$

where $\bar{E}$ is the available energy in the center of mass system, and

$$\bar{E}_f = \bar{E}_i - Q\,. \quad (11)$$

From Eqs. (10) and (11) one obtains the sum $\frac{1}{2}\theta_i + \frac{1}{2}\theta_f$, which is taken to be the effective angle at which the light product of the transfer reaction is observed. Note that this approach differs from that of Ref. 40, where it is assumed that $\theta_i \approx \theta_f$; these angles can be quite different in Eq. (10), depending on the Q value of the reaction.

This model was used to determine values of E_R and θ_R for transfers in which either ^{4}He or ^{3}He are the resulting light nuclei. The calculations are compared with the recoil data in part (b) of Fig. 9. A distance of closest approach of 14 fm, equivalent to $r_0 = 1.65$ fm, was used to match up the incoming and outgoing trajectories. The Q values were selected so that, in each reaction, sufficient excitation energy would be available in the Cf transfer product to evaporate neutrons and reach ^{245}Cf (dashed curves) or ^{244}Cf (solid curves). We see that the calculated curves are again consistent with the transfer of a Be cluster from ^{12}C to ^{239}Pu. Clearly, the detailed forms of the curves, and the masses of the He nuclides involved, are different in Figs. 9(a) and 9(b). So, trying to interpret such recoil data solely in terms of one particular model of transfer reactions may lead to equivocal results; yet the similarity of the curves in parts (a) and (b) of Fig. 9 does indicate the importance of Coulombic scattering in the observed reactions.

E. Excitation energies

The two-step model described by Eqs. (4)–(9), in contrast to that given by Eqs. (10)–(11), does not explicitly take into account the Q value of the assumed transfer path. However, since the model predicts values of both the energy and angle, E_R and θ_R, of the heavy product for a particular transfer reaction, the system is kinematically determined.[64] Thus, one can calculate the Q for that reaction path, from which the available excitation energy, E_x, is gotten with the relation[40]

$$Q = Q_{gg} - E_x\,; \quad (12)$$

here, Q_{gg} is the energy balance for the transfer, leaving the reaction products in their ground state. Since the light product of the transfer is assumed to have zero excitation energy, E_x becomes the excitation energy of the heavy product and can be compared, for each postulated transfer reaction ^{239}Pu(^{12}C, ^{A}He)$^{251-A}$Cf [Fig. 9(a)], with the energies required for emission of the appropriate numbers of neutrons to reach ^{245}Cf and ^{244}Cf (the possibility that the light fragment is also excited has been recently discussed in Ref. 65, but is not considered here). Gross disagreement between the calculated and experimentally required excitation energies would be proof of inconsistencies in the two-step model.

Such a comparison is shown in Fig. 10 where the heavy lines give the excitation energies for those (^{12}C, ^{A}He) transfers in which $A = 3$, 4, or 5. The dashed horizontal lines show the separation energies $S(xn)$ required to evaporate $x = 1$ to 5 neutrons from nucleus ^{247}Cf produced in the (^{12}C, ^{4}He) transfer[66]; similar $S(xn)$ values, differing by ~1 MeV from those in the figure, apply for the (^{12}C, ^{3}He) and (^{12}C, ^{5}He) reactions.

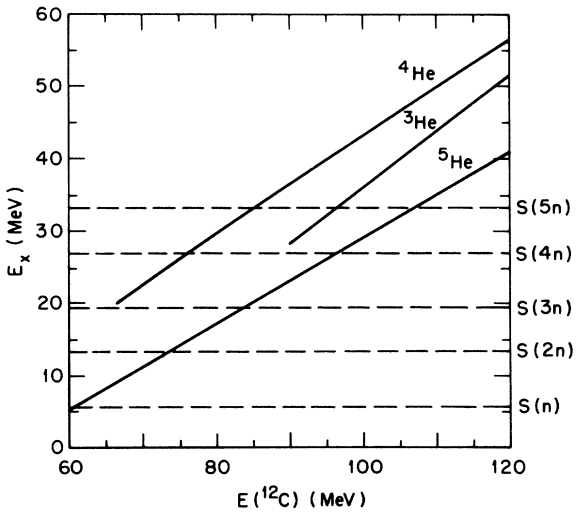

FIG. 10. Excitation energy E_x of the residual nucleus after the transfer process, as calculated with the two-step model for the reaction ^{239}Pu + ^{12}C. Only transfers in which the light product is a He isotope are considered. Horizontal dashed lines denote the separation energies $S(xn)$ for the emission of $x = 1$ to 5 neutrons from intermediate nucleus ^{247}Cf produced in the (^{12}C, ^{4}He) reaction (Ref. 66). Similar $S(xn)$ values, differing by ~1 MeV from those in the figure, apply for the (^{12}C, ^{3}He) and (^{12}C, ^{5}He) reactions.

The bombarding-energy interval to examine is that in which ^{245}Cf and ^{244}Cf were observed in the experiments, from ~60 to ~90 MeV. Figure 10 shows that the (^{12}C, ^{3}He) reaction does not contribute in this energy region. For the (^{12}C, ^{4}He) reaction, E_x varies from 20 to 37 MeV. The corresponding $S(xn)$ values for emission of two, three, and four neutrons from ^{247}Cf are 13.2, 19.3, and 26.9 MeV, respectively; the actual energies required are larger than these threshold values because the neutrons are emitted with kinetic energies of a few MeV, and some energy is also given off as radiation.[1] Thus, we conclude that the E_x values calculated for the (^{12}C, ^{4}He) reaction are in reasonable accord with the energies needed to reach the observed Cf isotopes. The same conclusion is reached when ^{5}He is the light fragment, and one to three neutrons are to be evaporated from ^{246}Cf.

A final point of interest about the two-step model is that the Q values calculated for the ^{239}Pu-(^{12}C, ^{4}He)^{247}Cf reaction are much closer to the Q-optimal values, obtained with the expressions containing recoil corrections in Ref. 40, than are the corresponding Q values computed for the production of either ^{3}He or ^{5}He. If the concept of an optimum Q value is correct for multinucleon transfers, the transfer of a ^{8}Be cluster is energetically favored.

IV. CONCLUSION

Measurements of the excitation functions, and of the range and angular distributions, of ^{245}Cf and ^{244}Cf produced with ^{239}Pu + ^{12}C clearly show that compound-nucleus processes are not involved in these reactions, in contrast to the results for ^{238}U-(^{12}C, xn) leading to the same products. The Pu + C data are consistent with the transfer of some aggregate from projectile to target, followed by the evaporation of neutrons.

The cross-section data indicate that $\sigma(\mathrm{C}, \alpha 2n\text{-}\alpha 3n) >> \sigma(\mathrm{C}, 2n\text{-}4n)$, a result that is ascribed to the much greater competition between fission and neutron emission in the Fm compound nuclei than in the Cf transfer products. As has been noted before (e.g., Ref. 50), knowledge of such differences in the yields of compound-nucleus and transfer reactions can be very important in optimizing experiments to produce isotopes of the heaviest elements.

The recoil data for ^{239}Pu + ^{12}C → ^{245,244}Cf are very different from those obtained for the compound-nucleus reactions ^{238}U + ^{12}C leading to the same products. For example, the recoil range or energy for Pu + C is 1.6 times the expected complete-fusion (CF) value at 67 MeV and decreases monotonically to 0.6 of the CF value at 97 MeV. And the most probable angle (centroid) for observing the Cf nuclides at energies well above the Coulomb barrier is ~17° for Pu + C, instead of 0° as expected for complete fusion.

A model in which the transfer reaction involves two steps, (1) transfer of a cluster, having the same velocity as the projectile, from projectile to target, followed by (2) Rutherford scattering of the remaining light nucleus and the resultant heavy nucleus, reproduces the trends exhibited by the recoil data; calculated average recoil energies, angles of emission, and excitation energies are in accord with the experimental results. The calculations indicate that the Cf nuclides are probably formed by transfer of Be from C to the Pu nucleus, with subsequent evaporation of neutrons to give ^{245}Cf and ^{244}Cf. However, computations with a somewhat different model of the transfer process, based only on the equations of Rutherford scattering, give results that differ, although not drastically, from the conclusions of the former model. Although scattering in the Coulomb field is important in both models, details of the momentum transfer involved in the transfer of nucleons from projectile to target are different. Thus, one must exercise some caution in interpreting recoil data such as are presented here. Systematic studies of transfer reactions, wherein the same products are observed from a variety of projectiles and/or targets, should help to elucidate the mechanistic details of such reactions.

An interesting by-product of recoil studies is that range and angular distributions can be used as aids in identifying new isotopes by distinguishing between compound-nucleus and transfer reactions. Such arguments have been put forth as support (e.g., Ref. 51) for discovery claims of elements 104 and 105. The present data and calculations indicate that the products of transfer reactions, although not very far removed from the compound nucleus (Cf rather than Fm), can still be distinguished from CN products. However, there are some intervals of bombarding energy where the recoil properties of both the transfer and complete-fusion reactions are rather similar, so that one must choose the experimental conditions carefully if recoil energies or angles are to be used to characterize new isotopes.

ACKNOWLEDGMENTS

We wish to thank Dr. T. Sikkeland and D. Lebeck for giving us copies of the programs for computing the cross sections of (HI, xn) and transfer reactions, and Dr. D. Guerreau and Dr. J. Galin, for the code based on Rutherford scattering [Fig. 9(b)]. Several lively discussions with Dr. T. Sikkeland

and with Dr. R. Bimbot and Dr. A. Fleury are also appreciated. Thanks are due J. Roberts for preparing the targets, P. Hammonds for performing the radiochemical separations, and to the ORIC operating staff for its customary help and cooperation. Finally, one of us (R.L.H.) wishes to thank Professor M. Lefort and the members of the Institut de Physique Nucléaire, Orsay, for their hospitality during an extended stay in which a part of this work was accomplished.

---

*Part of this work was done during a stay by R. L. H. at the Institut de Physique Nucléaire, Orsay, France.
†Operated by Union Carbide Corporation under contract with the U. S. Atomic Energy Commission.

[1]J. M. Alexander, in *Nuclear Chemistry*, edited by L. Yaffe (Academic, New York, 1968), Vol. I, Chap. 4.
[2]A. Zucker and K. S. Toth, in *Nuclear Chemistry* (see Ref. 1), Chap. 6.
[3]R. Kaufman and R. Wolfgang, Phys. Rev. 121, 192 (1961).
[4]J. B. J. Read, I. M. Ladenbauer-Bellis, and R. Wolfgang, Phys. Rev. 127, 1722 (1962).
[5]P. M. Strudler, Ph.D. dissertation, Yale University, 1966 (unpublished).
[6]P. M. Strudler, I. L. Preiss, and R. Wolfgang, Phys. Rev. 154, 1126 (1967).
[7]R. I. Morse and I. L. Preiss, Phys. Lett. 20, 509 (1966).
[8]J. M. Alexander and L. Winsberg, Phys. Rev. 121, 529 (1961).
[9]P. D. Croft, J. M. Alexander, and K. Street, Phys. Rev. 165, 1380 (1968).
[10]H. Kumpf and E. D. Donetz, Zh. Eksperim. i Teor. Fiz. 44, 798 (1963) [transl.: Soviet Phys.—JETP 17, 539 (1963)].
[11]E. Lozhynski, Nucl. Phys. 64, 321 (1965).
[12]R. Bimbot, D. Gardes, and M. F. Rivet, Phys. Rev. C 4, 2180 (1971).
[13]R. Bimbot, D. Gardes, and M. F. Rivet, Nucl. Phys. A189, 193 (1972).
[14]R. Bimbot and M. F. Rivet, Phys. Rev. C 8, 375 (1973).
[15]R. Bimbot, D. Gardes, R. L. Hahn, Y. de Moras, and M. F. Rivet, Nucl. Phys. A228, 85 (1974); and *Proceedings of the International Conference on Nuclear Physics, Munich, 1973*, edited by J. de Boer and H. J. Mang (North-Holland, Amsterdam/American Elsevier, New York, 1973), Vol. I.
[16]Y. T. Oganesyan, Y. E. Penionzhkevich, and A. O. Shamsutdinov, Yad. Fiz. 14, 54 (1971) [transl.: Sov. J. Nucl. Phys. 14, 31 (1972)].
[17]R. A. Williams, Ph.D. dissertation, Carnegie-Mellon University, 1972 (unpublished).
[18]Y. LeBeyec, M. Lefort, and M. Sarda, Nucl. Phys. A192, 405 (1972).
[19]H. Delagrange, A. Fleury, F. Hubert, and G. N. Simonoff, Phys. Lett. 37B, 355 (1971).
[20]F. Hubert, Ph.D. dissertation, University of Bordeaux, 1973 (unpublished).
[21]F. Hubert, H. Delagrange, and A. Fleury, Nucl. Phys. (to be published).
[22]A. Fleury, F. Mivielle, and G. N. Simonoff, Phys. Lett. 24B, 576 (1967).
[23]W. J. Knox, A. R. Quinton, and C. E. Anderson, Phys. Rev. 120, 2120 (1960).
[24]H. C. Britt and A. R. Quinton, Phys. Rev. 124, 877 (1961).
[25]R. M. Diamond, A. M. Poskanzer, F. S. Stephens, W. J. Swiatecki, and D. Ward, Phys. Rev. Lett. 20, 802 (1968).
[26]J. Galin, B. Gatty, M. Lefort, J. Peter, X. Tarrago, and R. Basile, Phys. Rev. 182, 1267 (1969).
[27]J. Galin, D. Guerreau, M. Lefort, J. Peter, X. Tarrago, and R. Basile, Nucl. Phys. A159, 461 (1970).
[28]D. Guerreau, thesis, 3rd cycle, University of Paris, Orsay, 1969 (unpublished), No. IPN-69-03-T.
[29]L. G. Moretto, D. Heunemann, R. C. Jared, R. C. Gatti, and S. G. Thompson, in Proceedings of the Third International Atomic Energy Symposium on the Physics and Chemistry of Fission, Rochester, 1973 (to be published).
[30]S. G. Thompson, private communication.
[31]A. G. Artukh, V. V. Avdeichikov, G. F. Gridnev, V. L. Mikheev, V. V. Volkov, and J. Wilczynski, Nucl. Phys. A176, 284 (1971).
[32]A. G. Artukh, V. V. Avdeichikov, J. Ero, G. F. Gridnev, V. L. Mikheev, V. V. Volkov, and J. Wilczynski, Nucl. Phys. A160, 511 (1970).
[33]A. G. Artukh, V. V. Avdeichikov, G. F. Gridnev, V. L. Mikheev, V. V. Volkov, and J. Wilczynski, Nucl. Phys. A168, 321 (1971).
[34]A. G. Artukh, G. F. Gridnev, V. L. Mikheev, V. V. Volkov, and J. Wilczynski, Nucl. Phys. A211, 299 (1973).
[35]A. G. Artukh, G. F. Gridnev, V. L. Mikheev, V. V. Volkov, and J. Wilczynski, Joint Institute for Nuclear Research Report No. JINR E7-6970, 1973 (unpublished).
[36]P. Colombani, H. Doubre, J. C. Jacmart, N. Poffé, M. Riou, J. C. Roynette, C. Stephan, P. P. Singh, and A. Weidinger, in *Proceedings of the International Conference on Nuclear Physics, Munich, 1973* (see Ref. 15).
[37]K. R. Greider, Annu. Rev. Nucl. Sci. 15, 291 (1965) and references contained therein.
[38]W. G. Simon and S. T. Ahrens, Phys. Rev. C 2, 1292 (1970).
[39]C. Toepffer, Phys. Rev. Lett. 27, 872 (1971).
[40]C. Toepffer, Z. Phys. 253, 78 (1972).
[41]P. J. Siemens, J. P. Bondorf, D. H. E. Gross, and F. Dickman, Phys. Lett. 36B, 24 (1971).
[42]D. M. Brink, Phys. Lett. 40B, 37 (1972).
[43]M. Kleber and R. Beck, Phys. Lett. 43B, 98 (1973).
[44]D. H. E. Gross, Phys. Lett. 43B, 371 (1973).
[45]E. K. Hyde, I. Perlman, and G. T. Seaborg, *The Nuclear Properties of the Heavy Elements* (Prentice-Hall, Englewood Cliffs, New Jersey, 1964), Vol. I, Chap. 5.
[46]E. K. Hyde, *The Nuclear Properties of the Heavy Elements* (see Ref. 45), Vol. III, Chap. 10.
[47]T. Sikkeland, N. H. Shafrir, and N. Trautmann, Phys. Lett. 42B, 201 (1972).
[48]T. Sikkeland, J. Maly, and D. Lebeck, Phys. Rev.

169, 1000 (1968).
[49]A. Ghiorso and T. Sikkeland, in *Proceedings of the Second United Nations Conference on the Peaceful Uses of Atomic Energy, 1958* (United Nations, Geneva, Switzerland, 1958), Vol. 15, paper No. P/2440.
[50]A. Ghiorso, M. Nurmia, K. Eskola, J. Harris, and P. Eskola, Phys. Rev. Lett. 24, 1498 (1970).
[51]G. N. Flerov, Y. T. Oganesyan, Y. V. Lobanov, Y. A. Lasarev, S. P. Tretiakova, I. V. Kolesov, and V. M. Plotko, Nucl. Phys. A160, 181 (1971).
[52]Hyde, Perlman, and Seaborg (see Ref. 45), Vol. II, Chap. 9.
[53]N. E. Holden and F. W. Walker, *Chart of the Nuclides* (Knolls Atomic Power Laboratory, General Electric Company, Schenectady, New York, 1972), 11th ed.
[54]Y. A. Ellis and A. H. Wapstra, Nucl. Data B3(No. 2) (1969).
[55]K. S. Toth, R. L. Hahn, M. A. Ijaz, and W. M. Sample, Phys. Rev. C 2, 1480 (1970).
[56]G. N. Flerov, S. M. Polikanov, V. L. Mikheev, V. I. Ilyushchenko, M. B. Miller, and V. A. Shchegolev, At. Energ. 22, 342 (1967).
[57]M. J. Nurmia, T. Sikkeland, R. Silva, and A. Ghiorso, Phys. Lett. 26B, 78 (1967).
[58]T. Sikkeland, A. Ghiorso, and M. J. Nurmia, Phys. Rev. 172, 1232 (1968).
[59]R. L. Hahn, Nucl. Phys. A185, 241 (1972).
[60]L. Winsberg and J. M. Alexander, Phys. Rev. 121, 518 (1961).
[61]P. G. Steward, University of California Report No. UCRL-18127, 1968 (unpublished).
[62]L. C. Northcliffe and R. F. Schilling, Nucl. Data A7, 233 (1970).
[63]R. J. Ascuitto and N. K. Glendenning, Phys. Lett. 48B, 6 (1974).
[64]R. D. Evans, *The Atomic Nucleus* (McGraw-Hill, New York, 1955), Chap. 12.
[65]J. P. Bondorf and W. Nörenberg, Phys. Lett. 44B, 487 (1973).
[66]W. D. Myers and W. J. Swiatecki, University of California Report No. UCRL-11980, 1965 (unpublished).